SUPPLEMENTAL METHODS

Immunocytochemistry.

Cardiomyocytes were plated on gelatin-coated glass coverslips. Cells were fixed in PBS containing 4% paraformaldehyde, permeabilized in PBS containing 0.3% Triton-X, and blocked with 5% BSA. Immunostaining was performed using anti-HA mouse monoclonal antibody (Sigma), anti-c-Myc rabbit polyclonal antibody (Sigma), anti-rat ANF rabbit polyclonal antibody (Phoenix Laboratories), anti-α-actinin mouse monoclonal antibody (Sigma), Alexa-fluor 488 goat anti-rabbit IgG (Molecular Probes), Alexa-fluor 594 goat anti-mouse IgG (Molecular Probes) and Vectashield mounting medium with DAPI (Vector Laboratories). Microscopic analyses were performed using fluorescence microscopy (Zeiss).

Co-Immunoprecipitation.

Preparation of immunoprecipitated samples has been described previously (1). Briefly, cell lysates were incubated with anti-HA antibody (Sigma), anti-c-Myc (Sigma) or mouse IgG (Sigma) overnight at 4°C. Immunocomplexes were precipitated using A/G sepharose (Santa Cruz) and proteins resolved by SDS-PAGE.

Luciferase assay.

The transcriptional activity of the ANF promoter was evaluated using an ANF-Luc reporter gene. Cells were transfected (Lipofectamine, Invitrogen) and luciferase activity determined (Promega) as described previously (2).

Immunohistochemistry.

Heart sections were stained with anti-phospho-Mst1/2 (T183/T180) rabbit polyclonal antibody (Abcam), anti-troponin-T mouse monoclonal antibody (Neomarkers), anti-TNF-α rabbit polyclonal antibody (Abcam), anti-Hsp47 mouse monoclonal antibody (Stressgen), Alexa-fluor 488 goat anti-rabbit IgG (Molecular Probes), Alexa-fluor 594 goat anti-mouse IgG (Molecular Probes) and Vectashield mounting medium with DAPI (Vector Laboratories). Microscopic analyses were performed using fluorescence microscopy (Zeiss).

Hemodynamic measurements.

Mice were anesthetized with 2.5% Avertin (0.29 mg/kg i.p.). Simultaneous recording of arterial pressures were obtained by using two pressure transducers, as follows: A 1.4-French catheter-tip micromanometer catheter (Millar Instruments) was inserted through the right femoral artery into the abdominal aorta. Then another 1.4-French Millar catheter was inserted through the right carotid artery into the ascending aorta and advanced into the LV, where pressures and the first derivative of LV pressure over time (dP/dt) were recorded. Arterial pressure gradients were measured as described previously (3).

SUPPLEMENTAL REFERENCES

1. Del Re, D.P., Miyamoto, S., and Brown, J.H. 2008. Focal adhesion kinase as a RhoA-activable signaling scaffold mediating Akt activation and cardiomyocyte protection. *J Biol Chem* 283:35622-35629.

2. Matsui, Y., Nakano, N., Shao, D., Gao, S., Luo, W., Hong, C., Zhai, P., Holle, E., Yu, X., Yabuta, N., et al. 2008. Lats2 Is a Negative Regulator of Myocyte Size in the Heart. *Circ Res* 103:1309-1318.

3. Hirotani, S., Zhai, P., Tomita, H., Galeotti, J., Marquez, J.P., Gao, S., Hong, C., Yatani, A., Avila, J., and Sadoshima, J. 2007. Inhibition of glycogen synthase kinase 3beta during heart failure is protective. *Circ. Res.* 101:1164-1174.

Supplemental Figure 1

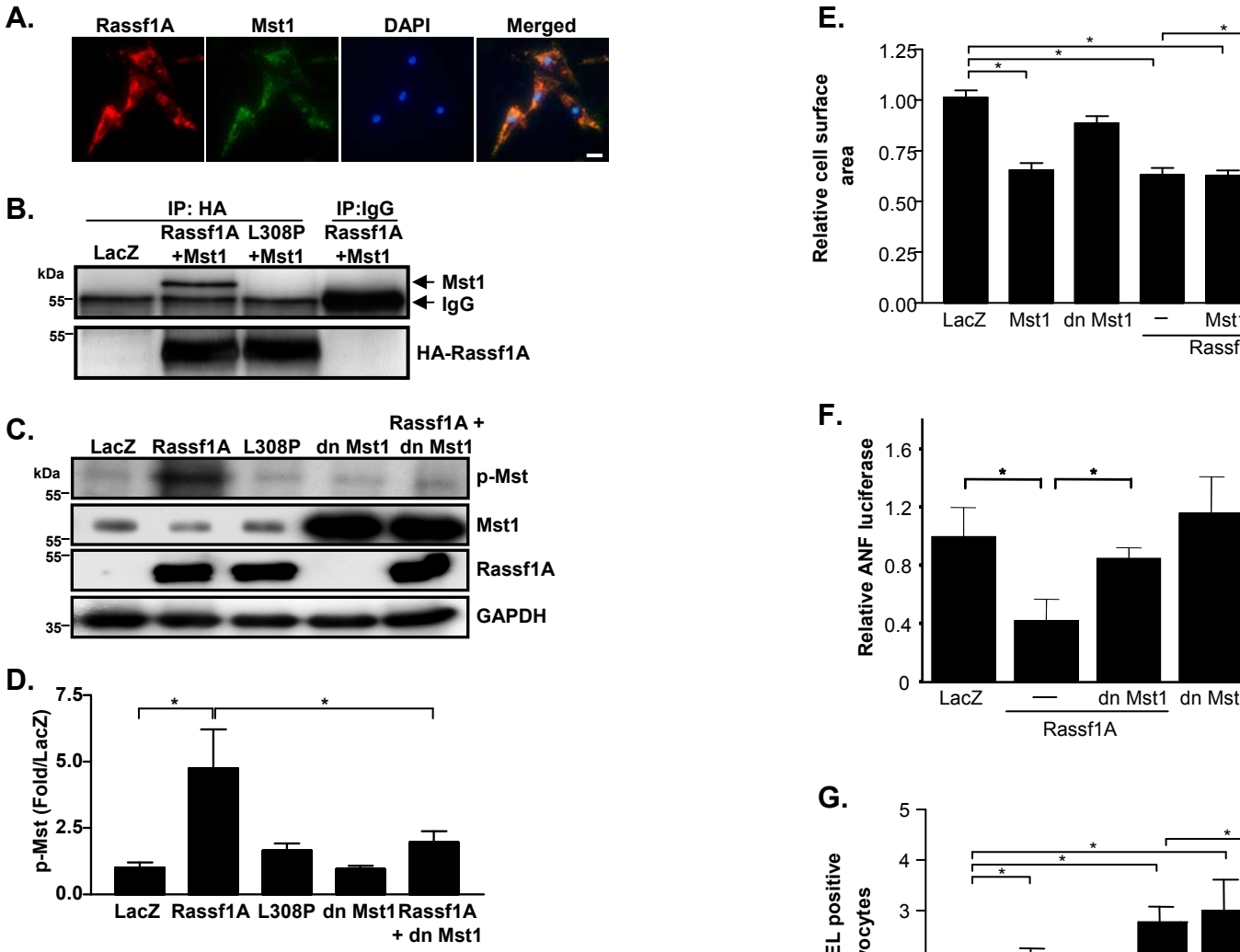

Rassf1A co-localizes with and activates Mst1 in cardiomyocytes. (**A**) Immunocytochemistry demonstrating co-localization of Rassf1A and Mst1 in neonatal rat cardiomyocytes. Representative images visualizing Rassf1A, Mst1, DAPI nuclear staining and merged are shown. Bar = 30 μm. (**B**) Immunoprecipitation assay demonstrating interaction of Rassf1A, but not mutant (L308P) Rassf1A, with Mst1 in cardiomyocytes. (**C,D**) Increased expression of Rassf1A, but not mutant (L308P) Rassf1A, activates Mst1 in cardiomyocytes. (**C**) Representative immunoblot. (**D**) Densitometric quantification of immunoblot analysis. dn Mst1 is kinase inactive (K59R) Mst1. *P<0.05. *n* = 3. (**E**) Cells were fixed and stained with α-actinin to visualize cardiomyocytes, and cell area was determined. *P<0.05. *n* = 3. (**F**) Luciferase reporter assay demonstrating inhibition of ANF expression by Rassf1A. *P<0.05, *n* = 3. (**G**) TUNEL staining was performed to quantify Rassf1A-induced apoptosis of cardiomyocytes. *P<0.05, *n* = 3. Data are averages ± s.e.m.

Supplemental Figure 2

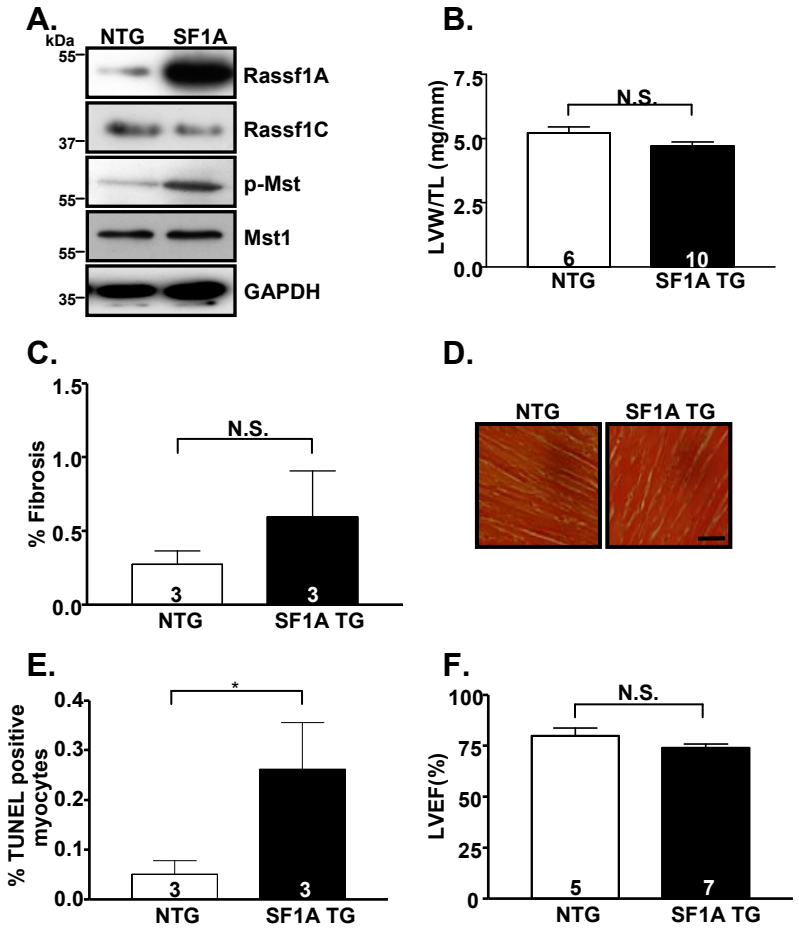

Cardiac-specific expression of Rassf1A activates Mst1 *in vivo*. (**A-F**) Baseline cardiac evaluation of adult Rassf1A transgenic mice. Animals were sacrificed at 10 weeks of age. (**A**) Representative immunoblot demonstrating transgene expression and Mst1 phosphorylation in the hearts of non-transgenic (NTG) and Rassf1A transgenic (SF1A TG) mice. (**B**) Left ventricular weight/tibia length (LVW/TL) ratio showed no significant difference in SF1A TG heart size. N.S. = not significant. (**C**) Fibrosis was assessed by Masson's Trichrome staining and fibrotic area determined. N.S. = not significant. (**D**) Representative images show similar extent of fibrosis. Bar = 100 µm. (**E**) TUNEL staining was used to quantify increased cardiomyocyte apoptosis in SF1A TG versus NTG hearts. *P<0.05. (**F**) Echocardiographic analysis showed no difference in left ventricular ejection fraction (LVEF%) between groups. N.S. = not significant. Data are averages ± s.e.m.

Supplemental Figure 3

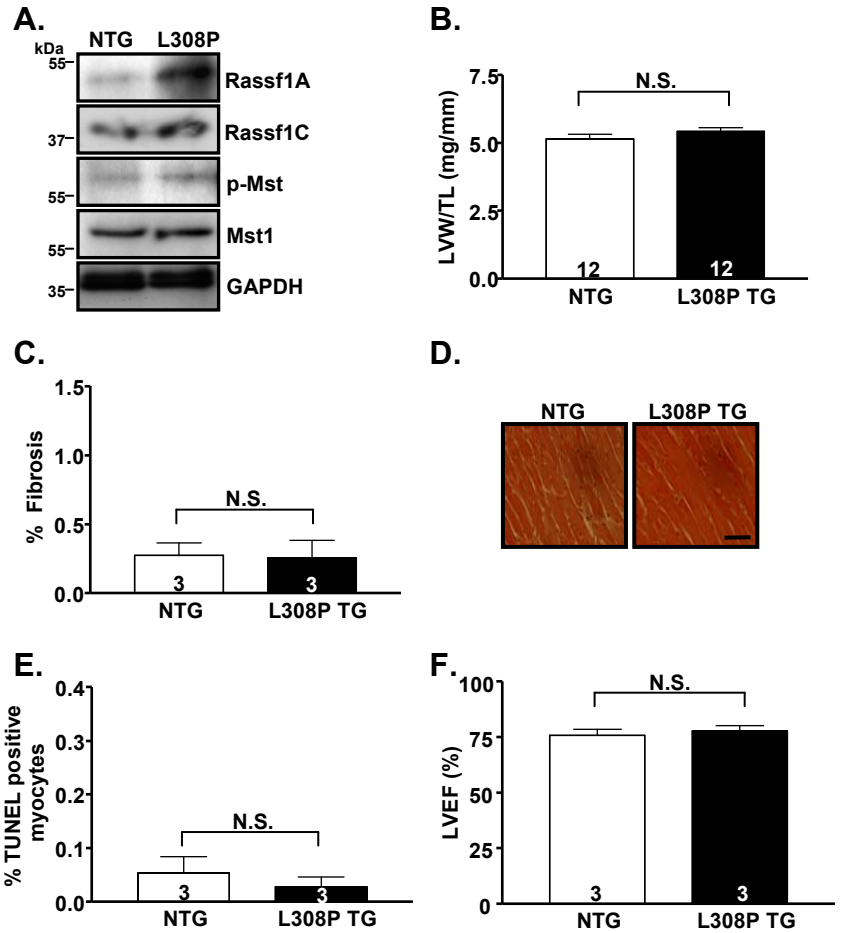

Cardiac-specific expression of (L308P) Rassf1A inhibits Mst1 activation *in vivo*. (**A-F**) Baseline cardiac evaluation of adult mutant (L308P) Rassf1A transgenic mice. Animals were sacrificed at 10 weeks of age. (**A**) Representative immunoblot demonstrating transgene expression and no increase in Mst1 phosphorylation in hearts from NTG and L308P TG mice. (**B**) Left ventricular weight/tibia length (LVW/TL) ratios show no difference between groups. N.S. = not significant. (**C**) Fibrosis was assessed by Masson's Trichrome staining and fibrotic area found to be comparable between groups. N.S. = not significant. (**D**) Representative images shown. Bar = 100 µm. (**E**) TUNEL staining was used to determine cardiomyocyte apoptosis. N.S. = not significant. (**F**) Echocardiographic analysis was performed and left ventricular ejection fraction (LVEF%) determined. N.S. = not significant. Data are averages ± s.e.m.

Supplemental Figure 4

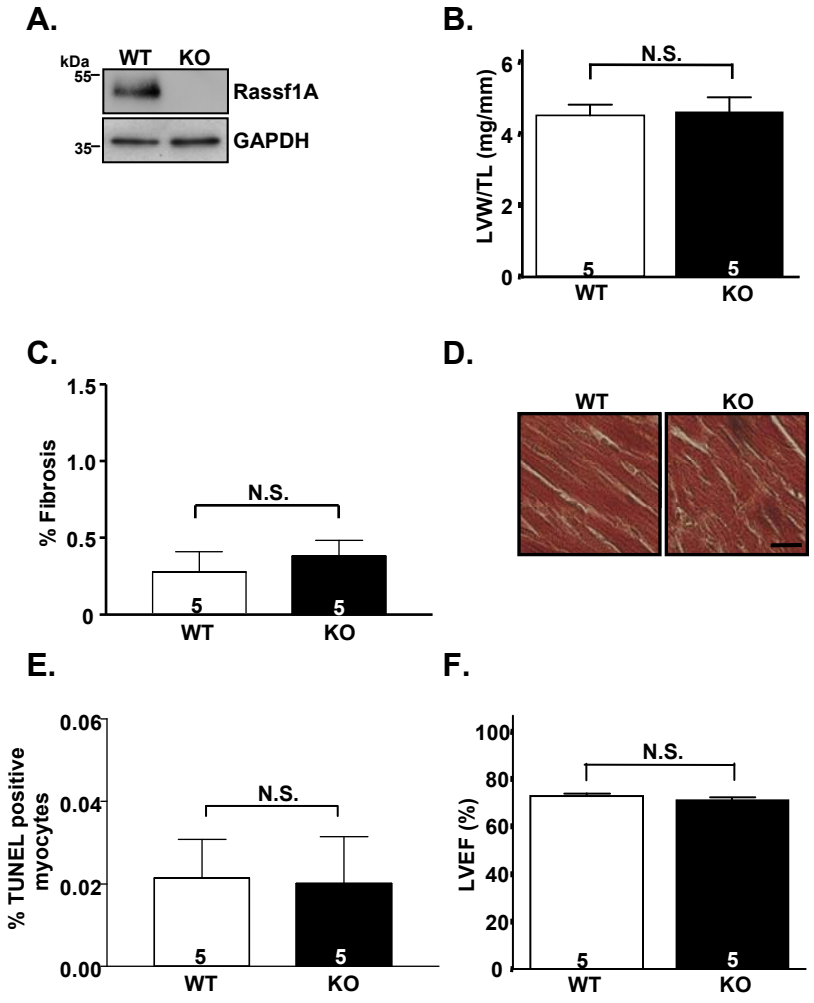

Baseline cardiac phenotype of *rassf1A* KO mice. (**A-F**) Baseline cardiac evaluation of adult *rassf1A* KO mice. Animals were sacrificed at 10 weeks of age. (**A**) Representative immunoblot demonstrating loss of Rassf1A expression in heart tissue from systemic knockout (KO) mice. (**B**) Left ventricular weight/tibia length (LVW/TL) ratios show no difference between groups. N.S. = not significant. (**C**) Fibrosis was assessed by Masson's Trichrome staining and fibrotic area was similar between groups. N.S. = not significant. (**D**) Representative images shown. Bar = 100 μm. (**E**) TUNEL staining shows no difference in cardiomyocyte apoptosis between WT and KO hearts. N.S. = not significant. (**F**) Echocardiographic analysis shows no difference in left ventricular ejection fraction (LVEF%) between groups. N.S. = not significant. Data are averages ± s.e.m.

Supplemental Figure 5

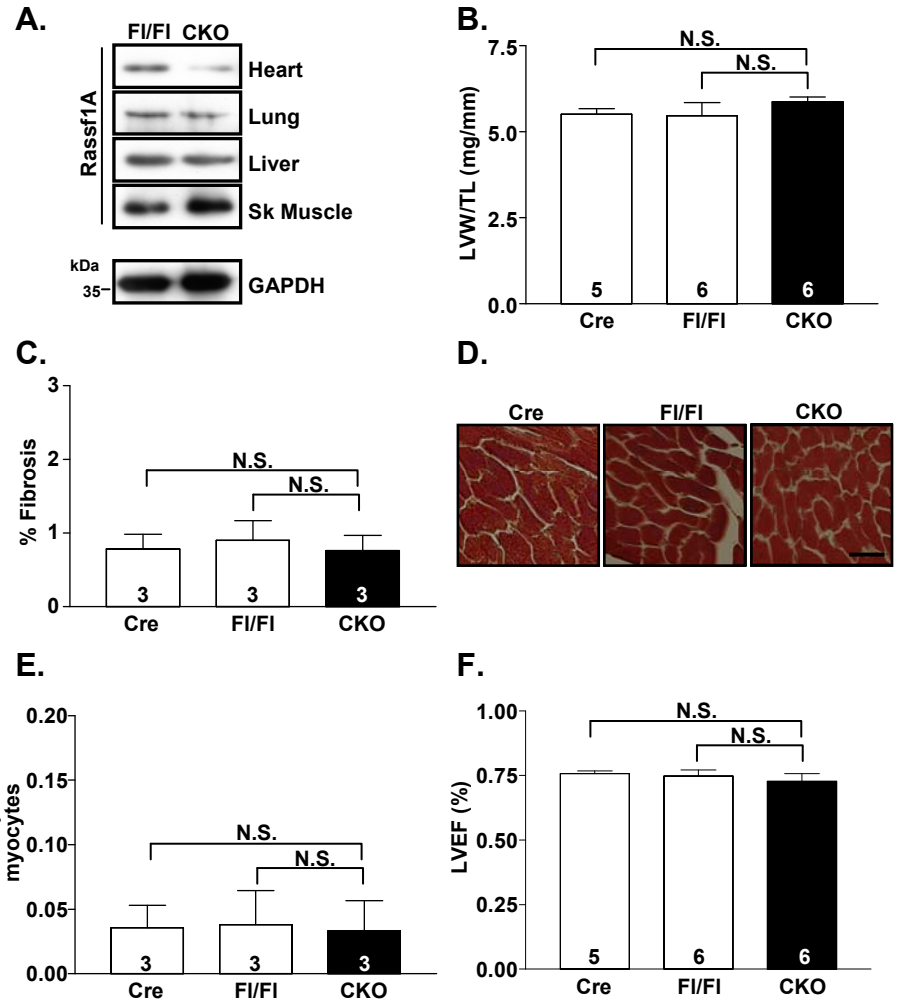

Baseline cardiac phenotype of *rassf1A* conditional KO mice. (**A-F**) Baseline cardiac evaluation of adult *rassf1A* CKO mice. Animals were sacrificed at 10 weeks of age. (**A**) Representative immunoblot demonstrating tissue specific depletion of Rassf1A expression in CKO heart. (**B**) Left ventricular weight/tibia length (LVW/TL) ratios show no difference between αMHC-Cre Tg (Cre), *rassf1A* $^{flox/flox}$ (Fl/Fl) controls and CKO mice. N.S. = not significant. (**C**) Fibrosis was assessed by Masson's Trichrome staining and was similar between groups. N.S. = not significant. (**D**) Representative images shown. Bar = 100 μm. (**E**) TUNEL staining shows no difference in cardiomyocyte apoptosis between groups. N.S. = not significant. (**F**) Echocardiographic analysis was performed and left ventricular ejection fraction (LVEF%) determined. N.S. = not significant. Data are averages ± s.e.m.

Supplemental Figure 6

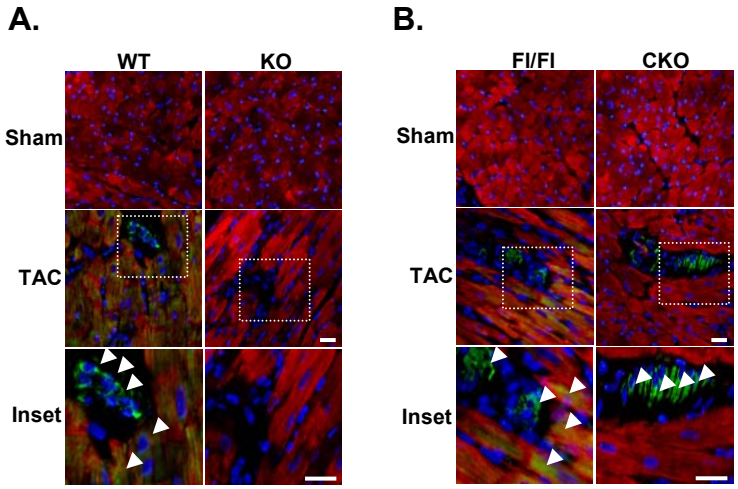

Endogenous Rassf1A in non-myocytes sustains Mst1 activation. Representative images detecting troponin T (red), phosphorylated Mst (green), and DAPI (blue) in WT and *rassf1A* systemic KO (**A**) and *rassf1A* $^{flox/flox}$ (Fl/Fl) and CKO (**B**) hearts. Bar = 100 μm.

Supplemental Figure 7

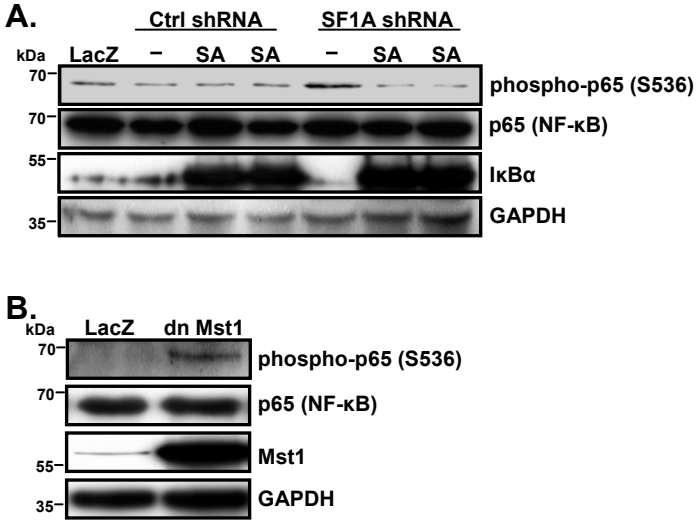

Rassf1A/Mst1 inhibits activation of the transcription factor NF-κB. Fibroblasts were isolated from neonatal rat hearts and passaged a minimum of three times prior to experimentation. (**A**) Representative immunoblot demonstrates that Rassf1A depletion increases phosphorylation of p65. Additionally, IκBαSA mutant (SA) expression is effective to prevent p65 phosphorylation following *rassf1A* knockdown. (**B**) Representative immunoblot demonstrating increased phosphorylation of p65 in response to dn Mst1 expression in cardiac fibroblasts.

Supplemental Figure 8

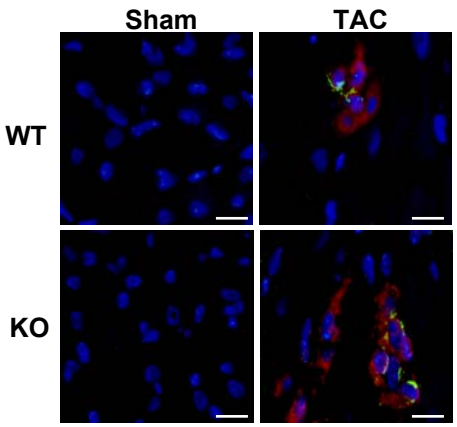

Cardiac fibroblasts mediate increased TNF-α expression in rassf1A KO hearts. Sham and TAC operated wild-type (WT) and *rassf1A* KO mouse hearts were sectioned and stained for Hsp47 (fibroblast marker, red) and TNF-α (green) using corresponding selective antibodies. Nuclei were stained with DAPI (blue). Increased double positive cells were observed in KO vs WT heart. Bar = 30μm.

Supplemental Table 1

	WT	KO
	(n=5)	(n=5)
HR	541 ± 27	501 ± 26
LSVP	101.6 ± 3.9	96.8 ± 3.2
LV +dp/dt	9100 ± 458	9200 ± 1179
LV -dp/dt	8500 ± 612	8400 ± 992
LVEDP	3.6 ± 1.2	2.8 ± 0.5
SBP	92.8 ± 5.9	94.0 ± 2.0
DBP	64.0 ± 5.9	70.0 ± 2.8
MBP	73.6 ± 6.0	78.0 ± 2.5

Supplemental Table 1. Baseline hemodynamic analysis of *rassf1A* KO mice.

Supplemental Table 2

	Cre	Fl/Fl	CKO
	(n=5)	(n=6)	(n=7)
HR	510 ± 13	518 ± 26	490 ± 20
LVSP	89.2 ± 2.7	91.3 ± 7.9	97.1 ± 5.9
LV +dp/dt	8960 ± 854	9200 ± 1997	7429 ± 670
LV -dp/dt	7120 ± 408	8067 ± 1395	7200 ± 629
LVEDP	4.6 ± 0.4	2.8 ± 1.0	3.7 ± 1.4
SBP	85.6 ± 5.2	90.0 ± 7.9	89.7 ± 4.2
DBP	53.6 ± 6.3	57.7 ± 5.2	56.6 ± 4.7
MBP	64.3 ± 5.8	68.4 ± 5.9	67.6 ± 4.4

Supplemental Table 2. Baseline hemodynamic analysis of *rassf1A* cardiomyocyte-specific KO mice.